Assessment of lake-level variations to decipher geological controlling factors and depositional architecture of Lake Fuxian, Yunnan Plateau: preliminary insights from geophysical data

Umar Ashraf · Hucai Zhang · Aqsa Anees · Xiaonan Zhang · Lizeng Duan

Abstract   Lake Fuxian is one of the deepest tectonic plateau freshwater lakes in the southeastern Tibetan Plateau, China. However, questions such as how old the lake is, how deep the total sedimentary thickness sequences are, and what landscape of the lake basin settings and geological structures are unknown. Here, based on fifteen seismic reflection profiles, we applied seismic facies and seismic sequence stratigraphic analyses to interpret the lake sequences. The results of the seismic response reveal that the maximum thickness of the sedimentation is ca. 1238 m and lies toward the NNE region of the lake basin on the L10-2 survey line. Lake sediments can be categorized into five seismic sequences and six seismic horizons. The oldest clinoforms in the deepest sequence (Sq-5) show that the depositional center was shifted to ~19 km from the NNE region to the SSW modern location and was ~930 m lower than the current lake floor. Multiple and complex tectonic activities strongly impacted on the lake basin, and a series of normal faults created an overall crustal extensional regime, resulting in the formation of many horst and graben structures.

Article highlights

- Five sequences and fourteen seismic facies are categorized in lake basin.
- Coastline migrated ~19 km to SSW in northern basin of its current location.
- Maximum thickness towards south is 303m on L3 and 1238m on north at L10-2.
- Tectonic activity played important role in forming horst-graben structures.
- Major controlling factors are tectonics, subsidence & sedimentary thickness.

U. Ashraf · A. Anees (✉)
Institute of International Rivers and Eco-Security, Yunnan University, Kunming 650500, China
e-mail: aqsaanees@ynu.edu.cn

U. Ashraf · H. Zhang (✉) · A. Anees · X. Zhang · L. Duan
Institute for Ecological Research and Pollution Control of Plateau Lakes, School of Ecology and Environmental Science, Yunnan University, Kunming 650500, China
e-mail: zhanghc@ynu.edu.cn

H. Zhang
Southwest United Graduate School, Kunming 650092, China

1 Introduction

The ecosystems of plateaus are significantly impacted by the presence of rift lakes (Zhang et al. 2021). Additionally, they provide a foundation for the continued social and economic growth of plateaus (Zhuo

et al. 2021). Lakes are highly important for ecological and biochemical processes; therefore, comprehending the depositional patterns, lake-level changes, distributions, and stratigraphic and structural variations is highly important (Messager et al. 2016). In China, there are approximately 2700 lakes, 70% of which are located in high plateau areas (Zhang and Yang 2012). The Yunnan Plateau, which is situated in southwestern China, has an average elevation of approximately 2000 m and contains numerous natural lakes (Wang et al. 2018). Within the Yunnan Province, there are nine major plateau freshwater tectonic lakes. These include Lakes Dianchi, Erhai, Lugu, Yangzonghai, Yilong, Xingyun, Chenghai, Qilu, and Fuxian (Cheng et al. 2020) (Fig. 1a). Lake Fuxian is located toward the southeastern region of the Yunnan Province of China, and has enormous importance due to its large volume within the great lakes of the Yunnan Plateau. Lake Fuxian contains 72.8% of the total volume of the Yunnan Plateau's nine large tectonic lakes, or 9.16% of China's freshwater lakes (Dai et al. 2017).

Lake data on the Tibetan Plateau serve as a significant repository of climate and environmental fluctuations (Zhang et al. 2021a, b; Gao et al. 2024). Recently, late Cenozoic sedimentation and depositional patterns in East African lake basins have been utilized to explain ancient rift basin stratigraphy (Flannery and Rosendahl 1990; Johnson et al. 1996, 2002; McGlue et al. 2008). In another study, the author studied some of the deepest and most aerially widespread lake layers on Earth that are preserved in the Permian deposits of the Junggar and Turpan-Hami Basins in the Xinjiang Province of Northwest China (Wartes et al. 2000). In a recent study, the authors studied the paleoseismic records of Hasuhai Lake in Inner Mangolia, North China (Wang et al. 2021a, b). However, no studies have been conducted on the rift lakes of southwestern China. Many studies are available related to the environmental aspects of Lake Fuxian. These studies are related to the following factors related to organic carbon burial in rift lakes: spatial–temporal changes, sources, and driving variables of organic carbon burial (Zhuo et al. 2021; Yin et al. 2021); sources of heavy metal pollutant pollutants (Zeng and Wu 2009); distributions of macrozoobenthos (Cui et al. 2008); phytoplankton responses to solar Ultravoilent radiation (Zhang et al. 2021a, b); and effects of geographical variation on land-use patterns (Dai et al. 2017). However, few studies related

to the geological aspects of Lake Fuxian are available. These studies have focused mostly on modern sedimentation rates for more than a century (Wang et al. 2018) and for the last 150 years (Wang et al. 2011; Wang et al. 2021a, b). In a recent study of the Chinese literature, the authors studied the mineral composition, carbonate content, and lake-level changes over the last 12 ka and their relation to the climate within Lake Fuxian (Li et al. 2019a, b). However, no geophysical study has been conducted within the Lake Fuxian basin. Compared with the other aspects of the lake sediments of the Yunnan Plateau tectonic lakes, no attention has been given to the geophysical exploration of Yunnan lakes, SW China. This is especially true when comparing this study with dedicated research on other sedimentary rocks within SW China. Therefore, comprehensive research on Lake Fuxian is highly important and imperative.

Sediments within rift lakes provide useful information related to the distribution of structural cum stratigraphic changes, climate variations, and lake evolution (Zhuo et al. 2021). Tectonic activities and climatic changes are the main controlling factors for lake-level variations within tectonically active rift basins. Therefore, these two factors should be considered when interpreting geological models of rift basins using seismic sequence stratigraphic modeling (Strecker et al. 1999). It is a quite problematic and challenging task to map a robust contemporary analog for a whole paleolake rift basin. However, the ancient stratigraphic records of continental rift basins can typically be resolved in great detail with the help of high-quality seismic reflection data, which also makes it possible to apply seismic sequence stratigraphic concepts to basins filled with tectonic rift basins (Scholz et al. 1990). Modelling of the tectonic history generated using multichannel seismic data from the Baikal rift zone suggested that the process of crustal extension in rift zones often involved a sequence of slow rifting and subsidence, followed by rapid rifting and intensified tectonic activity (Hutchinson et al. 1992). In another study, the authors successfully interpreted the three main lake-level cycles through seismic profiles and drilling cores in Lake Malawi (Lyons et al. 2011). Therefore, we have employed seismic sequence stratigraphy as an advanced and effective tool to attain a higher level of accuracy in the categorization of facies distributions and depositional

architectural interpretations (Ashraf et al. 2019, 2021; Anees et al. 2022). Seismic sequences display internal and cyclical stacking packages of seismic reflections that are interpreted as the stratigraphic response of a lowstand paleolake to tectonism (forced regression). However, successful lake-level rebuilding is associated with transgressive and highstand system tracts (Strecker et al. 1999).

In this pioneer geophysical study of Lake Fuxian, we aim to construct a detailed framework established through the interpretation of seismic reflection profiles to comprehend the vast geological structure of the lake in the Fuxian Basin. We employ geophysical analyses to analyze the sedimentary characteristics and geological meaning of the sedimentological response to variations in lake level. We also aim to analyze the sedimentary thickness, extent of spatial and vertical distributions of hidden faults, and the deep depositional architecture of the lake basin to determine the geological controlling factors by assessing lake-level variations and sequences. The literature on drill cores within the uppermost sequence (~ 3 m) published by Li et al. (2019a, b) proved to be useful in developing a reliable interpretation.

1.1 Research gaps and motivation

Compared with the environmental aspects of the lake sediments of the Yunnan Plateau tectonic lakes, comparatively little attention has been given to the geophysical exploration of Yunnan lakes in SW China. Therefore, comprehensive geophysical research must be conducted on Lake Fuxian. The purpose of this study was to explore the research gaps present among the deepest freshwater lakes within the Yunnan Plateau through geophysical study. This research aims to fill the following significant research gaps;

1. The geophysical understanding of Lake Fuxian has yet to be explored. There is no published literature on the Lake Fuxian using the deep-water multichannel seismic exploration data. Additionally, the former understanding of the deep stratigraphic structure was limited mainly to the reference of the stratigraphic structure of the lake shoreline of Lake Fuxian.

2. Understanding sediment thickness is fundamental to exploring the crustal structure, sedimentary loading and long-term sedimentation rates of a basin. However, the exact thickness distributions within the southern, central and northern basins are still unknown.

3. The depositional settings of the Lake Fuxian basin need to be adequately addressed to describe the spatial and vertical distributions of the unknown stratigraphic sequences.

4. What are the controlling factors that influence the mechanism of crustal extension and the formation of horst-graben structures? Additionally, what are the effects of seismicity and lake-level variations on the sedimentation rates?

2 Geology of the study area

2.1 Topography

Lake Fuxian (102° 49′–102° 57′ 7 E, 24° 21′–24° 38′ 8 N) is a north−south trending karst rift lake shaped like an inverse gourd and located in Yuxi city is 70 km (43 mi) away from Kunming (Dai et al. 2017) (Fig. 1b). Lake Fuxian is the deepest lake within the Yunnan Plateau region (Cui et al. 2008) and the third deepest freshwater oligotrophic lake in China (Zhang et al. 2021a, b). The lake has a storage capacity of 18.9 billion cubic meters. It is approximately 31.5 km long from north to south and narrow in the middle, with a width of approximately 11.5 km in the north and a width of approximately 3.2 km in the south. The water depth is deep in the north and shallow in the south, and the average water depth is approximately 89.6 m, with a maximum depth of 157.5 m (Fig. 1c) (Zeng and Wu 2009). The nearshore lake bottom on both sides is steep, but the slope becomes gentle below a water depth of 50 m and becomes flatter below 100 m. The runoff area of the basin is 1053 km². It covers an area of 211 sq. km (81 sq. mi), and the maximum depth is 155 m (508 ft.), making it the third deepest freshwater oligotrophic lake in China (Zhang et al. 2021a, b). More than 100 rivers flow into Lake Fuxian, and the water is discharged outside from a single outlet (Zhang et al. 2021a, b).
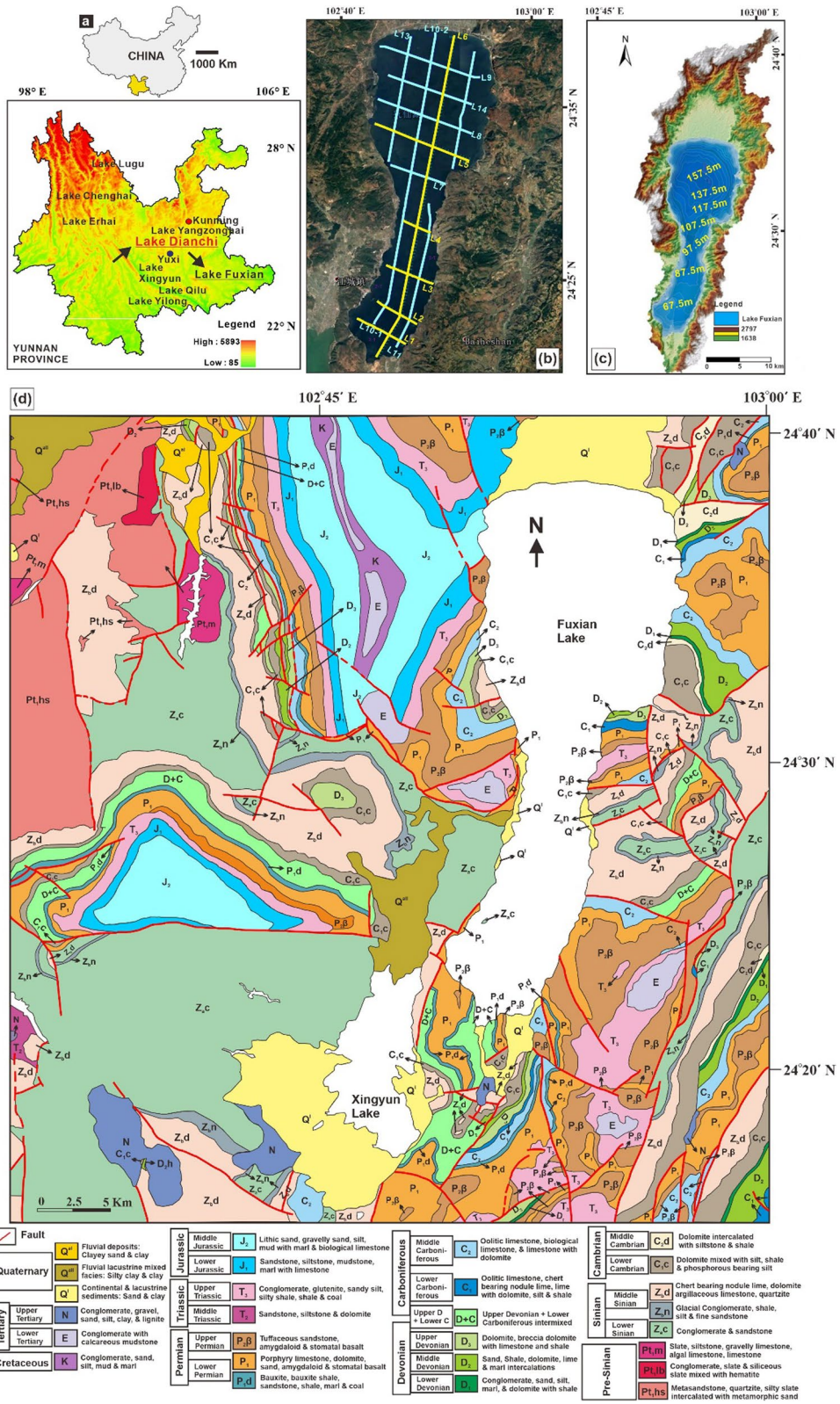
2.2 Tectonics and structure

Lake Fuxian is located in the basin range area of the Yunnan-Guizhou Plateau in the southeastern Tibetan Plateau (Zhang et al. 2021a, b). The geotectonics of Lake Fuxian belong to the intersection of the Yangtze paraplatform, South China fold system and Lanping-Simao fold system (Bureau of Geology and Mineral Resources of Yunnan Province 1990). In terms of the geological structure, Lake Fuxian is located on the Xiaojiang Fault (XJF). The XJF formed during the Jinning period in the Proterozoic. The main fault zone crossing Lake Fuxian is sinistral, with a horizontal offset of 2.5–3.0 km (Wang et al. 2009). The fault rupture of the XJF, it can be divided into three parts according to its geometric characteristics and features (Jun et al. 2003). The northern part is a simple fault and consists of Qiaojia to Menggu, which are approximately 50 km long. However, the middle to southern part has numerous complicated minor faults. The southern part comprises two parallel branch faults ~15 km apart, referred to as the east and west branches (Cheng et al. 2021). Lake Fuxian is a part of the Chengjiang Basin, a faulted structural lake basin controlled by the western branch of the southern section of the XJF. The southern part of the XJF contains numerous small-scale faults near Lake Fuxian and Lake Qilu, reflecting an overall extensional tectonic stress regime (Jun et al. 2003; Li et al. 2019a, b; Cheng et al. 2021).

The Xiaojiang and Qujiang faults are developed in the southeast and southwest corners, respectively, whereas the Puduhe fault and Yujiang fault run through them in the west. The neotectonic movement in the study area is strong and includes rifts along faults, differential uplifts and downs of fault blocks, strike-slip faults and numerous seismic events (Wang et al. 2009). The fault cliffs on both sides of the lake are high-angle normal faults, and the secondary faults on both sides are distributed in a feather shape, with a horizontal offset of 2.0 km. The XJF has been active many times since the Neogene. A series of late Cenozoic basins, such as Dongchuan, Yanglin, Yiliang, Chengjiang, and Jiangchuan, and modern lake basins, such as Lake Yangzong, Lake Fuxian and Lake Xingyun, are developed along the fault zone. Since the Quaternary, the XJF has been characterized by a strong left-lateral strike-slip fault, and its western branch fault has shown noticeable tension and torsion (Nanjing Institute of Geography and Limnology 1990). The differential movement on both sides reaches 7.5 ± 3.8 mm/a, which is one of the significant signs of Holocene tectonic activity, with more than 10 earthquakes of $M \geq 6$ occurring alongside the XJF seismic belt (Wang et al. 2009; Guo et al. 2021).

2.3 Stratigraphic settings

According to lithology classification, there are three main types of strata exposed around the Lake Fuxian basin (Bureau of Geology and Mineral Resources of Yunnan Province 1990):

1. Limestone and dolomite, with a distribution area of 159 km^2;
2. Shales and conglomerates, with an area of 159 km^2;
3. Basalt, with a distribution area of approximately 55 km^2.

According to the regional geological data, sedimentary rocks are the most common in the study area, lacking Ordovician and Silurian rocks. The bedrock around Lake Fuxian is mainly Sinian, Cambrian, Devonian, Carboniferous, Permian, Triassic and Jurassic (Fig. 1d). The lithologies of the different formations during their periods are described below from older to younger strata as follows:

The Sinian ($Z_a c$, $Z_b n$, $Z_b d$, $Z_b dn$) system is dominated by grayish purple-grained feldspar lithic sand, glacial conglomerate and dolomite. The Cambrian ($C_1 q$, $C_1 c$, $C_1 l$, $C_2 d$) strata are dominated by light black dolomite with intercalations of siltstone

and shale. The Devonian rocks (D_1, D_2, D_2h, D_3) are dominated by dark gray dolomite, red sandy limestone and calcareous mudstone. The Carboniferous (C_1y, C_1dw, C_1ds, C_2w and C_3m) strata consist of gray oolitic limestone, siltstone and black shale. The Permian rocks (P_1d, P_1q, P_1m, $P_2\beta$) comprise gray black basalt, yellow bauxite shale and coal seams. The Triassic (T_2, T_3p, T_3g and T_3s) system is dominated by sandstone and silty shale. The Jurassic (J_1f, J_2z, J_2s, J_2t) system is composed of yellowish white sandstone, reddish siltstone and calcareous mudstone. The Cretaceous (K) system is composed of sandstone, conglomerate and muddy siltstone. The Paleogene (E) strata are mainly composed of red conglomerate and calcareous mudstone. The overburden is composed of Neogene and Quaternary rocks. The Neogene (N) rocks are dominated by lake facies and swamp facies sedimentation, and their lithology is mainly composed of lignite, sandy gravel, and silt intercalated with sandy clay. The Quaternary sediments (Q^1, Q^{all}, and Q^{al}) are dominated by lake sedimentation, and their lithology is composed of clay, fine sand, and sandy gravel (Nanjing Institute of Geography and Limnology 1990).

3 Data and methods

3.1 Acquisition and processing of seismic reflection profiles

To comprehend the ancient seismic records of Lake Fuxian, the Jiangsu Geological Exploration Technology Institute, Nanjing (JSGETI), undertook a multichannel seismic exploration survey on Lake Fuxian in collaboration with the Institute for Ecological Research and Pollution Control of Plateau Lakes, Yunnan University. The design, evaluation work, and processing of the survey were completed in two phases. Initially, the first six seismic lines (L1–L6) were collected during October 2018. In the second phase, nine additional seismic lines (L7–L14) were collected during October 2021. The total length of the completed survey and the survey orientations are shown in Table 1. A total distance of 154.3 km^2 of digital, poststacked 2D seismic data was available for this study. The data were collected in such a way that dip lines such as Line-6 were orthogonal to the horst-graben system of the Lake Fuxian basin. These include 9 nearly WNW-ESE-oriented and 6 SSW-NNE-oriented seismic profiles.

Table 1 Summary of the dataset showing the orientations, coordinates and lengths of the seismic survey lines

Line number	Direction	Starting point		End point		Completion length (m)	Total distance (m)
		X	Y	X	Y		
L1	WNW−ESE	2,696,806.47	588,370.14	2,699,197.60	583,887.64	5011.5	154,274
L2	WNW−ESE	2,698,631.92	589,404.37	2,700,742.51	585,752.87	4237.5	
L3	WNW−ESE	2,702,343.00	590,898.94	2,704,057.66	586,557.40	4696.5	
L4	WNW−ESE	2,707,053.74	590,530.76	2,708,102.92	588,209.64	2554.5	
L5	WNW−ESE	2,713,634.88	594,184.20	2,717,066.85	585,520.71	9331.5	
L6	SSW−NNE	2,725,143.23	592,811.27	2,695,676.90	585,660.77	30,553.5	
L7	WNW−ESE	2,713,259.14	586,940.49	2,711,513.08	591,976.29	5345	
L8	WNW−ESE	2,719,320.83	585,793.55	2,716,124.75	594,386.89	9183	
L9	WNW−ESE	2,724,130.73	586,007.62	2,721,297.11	595,206.44	9679	
L10-1	SSW−NNE	2,698,643.65	585,475.66	2,713,076.14	588,948.68	15,031	
L10-2	SSW−NNE	2,711,721.91	588,714.04	2,725,427.83	591,047.47	13,927	
L11	SSW−NNE	2,696,526.17	587,475.71	2,709,759.59	590,525.86	13,767	
L12	SSW−NNE	2,712,933.65	592,653.93	2,723,698.51	594,686.43	10,999	
L13	SSW−NNE	2,713,472.84	586,850.58	2,725,081.59	588,789.04	11,823	
L14	WNW−ESE	2,721,517.48	586,751.28	2,718,809.98	594,413.27	8135	

Table 2 Summary of the acquisition and processing survey parameters

Multichannel seismic-reflection survey parameters	
Years	October 2018 (L1–L6) & October 2021 (L7–L14)
Total acquisition distance (km)	154.3 km
Channel spacing	2 m
Source	Mini-G Air Gun (France) & GS-1.2/250 air compressors
Acquisition system	GEO-SENSE LW 48 channel(Netherland)
Receiving system	48 floating detection cables (2 m apart)
Excitation energy	18Mpa
Excitation interval	4 s
Air gun water depth	4 m
Cable water depth	1.5 m
Recording length	1024 ms
Sampling rate	0.5 ms
Offset	30 m
Routine processing	Promax software—spectrum analysis → frequency filtering → velocity scanning → NMO correction and stacking
Postprocessing	Prediction deconvolution → residual static correction → multiple velocity analysis → poststack deconvolution → poststack migration → & poststack denoising
Positioning/navigation	Zhonghaida iRTK5 satellite differential GPS

The procedure for acquiring and processing field information is as follows: the seismograph utilized in the study was tobtained from the GEO-SENSE LW 48 (Netherlands) channel seismic acquisition system. The source employed during the survey included two GS-1.2/250 (France) air compressors and the double gun combination of the Mini G air gun. To ensure the authenticity of the received signal, passband reception was utilized in this work. The technical parameters, incorporating the source and receiver parameters, are presented in Table 2. To process the data, Landmark Promax processing software was used to improve the signal-to-noise ratio of the seismic data. The seismic data utilized in the study are poststacked time-migrated seismic profiles stored in SEG-Y format.

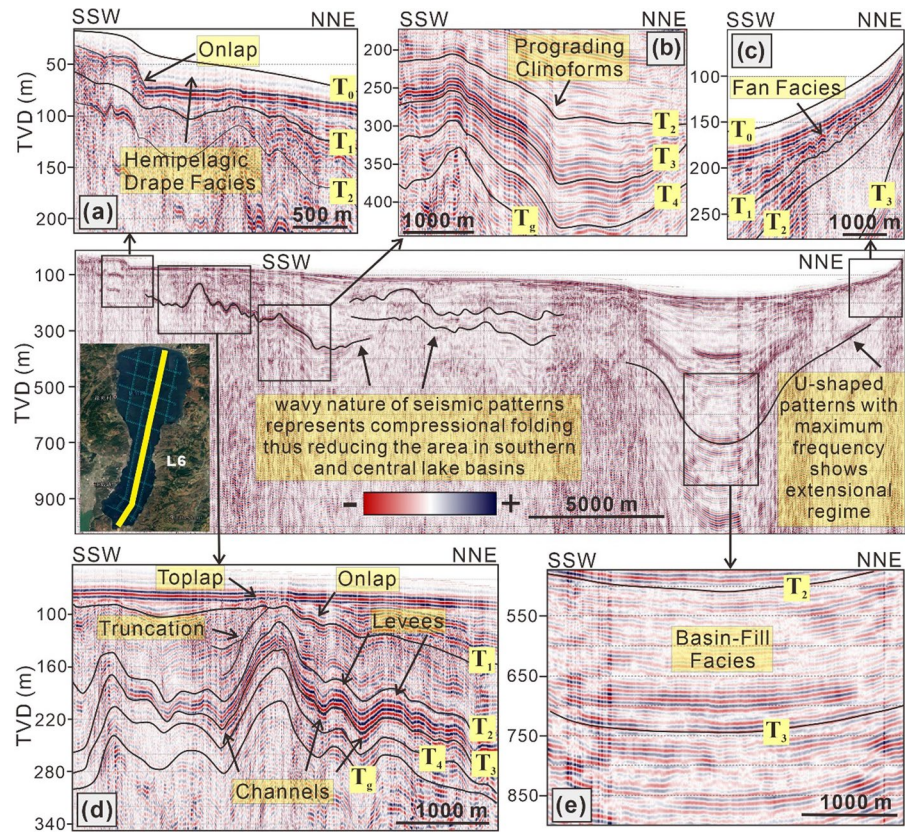### 3.2 Stratigraphic and paleobathymetric interpretation

The average velocities of each seismic profile were also available and were processed in HRS interpretation software to convert the time sections to depth sections. The depth sections were loaded in two software programs. The Fugro Jason™ Geoscience Workbench (JSW) and the Petrel™ E&P software suite from Schlumberger and CGG are used for further interpretation of horizons and fault markings. Initially, a basemap was established by utilizing the navigation and SEG-Y datasets to highlight the geometry and orientation (dip and strike) of the seismic profiles. Seismic sequence stratigraphy and seismic facies analysis are performed for detailed interpretation of paleoseismic records of the basin. Later, the interpretations were manually marked using Corel Draw graphics software to present a detailed interpretation of the depositional sequences, stratal terminations and fault markings.

3.3 Seismic sequence stratigraphy

The interpretation approach was concentrated on building a comprehensive stratigraphic framework by employing the methodology of seismic sequence stratigraphy for the Lake Fuxian basin, as employed for the lacustrine strata (Bohacs et al. 2000). Seismic stratigraphic analysis was performed utilizing the Petrel interpretation software. The principles of sequence stratigraphy were employed to map depositional sequences via the identification of stratal terminations on seismic profiles (Lyons et al.

Fig. 2 Categorization of basic seismic facies interpreted on the L6 survey line. The seismic reflection characteristics of the **a** hemipelagic drape facies, **b** progradational delta facies, **c** fan facies, **d** channel-levee fluvial facies, and **e** basin-fill lacustrine facies

4 Results

4.1 Seismic facies analysis

Several types of facies patterns were recognized on seismic sections in the basin. Several authors in the literature have recognized the seismic facies pattern on seismic reflection profiles of lakes at the regional level (Colman et al. 2003; Bohacs et al. 2000; Mcglue et al. 2008; Lyons et al. 2011). By analyzing and comparing the external geometry, amplitude, frequency, and continuity of the reflected wave groups of the seismic time profiles of each survey line, the effective reflected wave groups and their obvious anomalies,

2011). Several sequence boundaries are marked as horizons showing onlap patterns or truncation of reflections. Furthermore, these mapped horizons may show the characteristics of flooding surfaces marked by downlap patterns on seismic sections (McGlue et al. 2008).

such as faults, were delineated. Moreover, the geophysical data results were combined with regional geology data to determine the stratigraphic structure, sedimentary characteristics, and faulted strata to provide detailed information for the study of the Lake Fuxian basin. We have presented an abridged form of seismic facies types, which are as follows:

Hemipelagic drape facies are composed of straight parallel reflections with high continuity and medium amplitude and form an onlapping pattern on the pre-existing reflections of the lake floor (Fig. 2a). In addition, these facies usually overlie the steeply dipping pattern of clinoform sets. These facies include detrital clay and silt along with interbedded amounts of silica and organic matter (Johnson et al. 2002).

The progradational delta facies are composed of steeply dipping sigmoid-shaped reflections with low continuity and low amplitude (Fig. 2b). There are reflections toplap on the upper surfaces and downlap on the lower surfaces. These facies are composed of relatively coarse-grained gravels and sand (Butch 1996).

Table 3 A concise classification of seismic facies (SF) showing the graphical presentation, reflection features, and their geological significance and interpretation
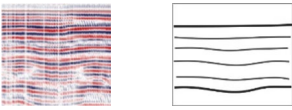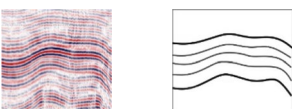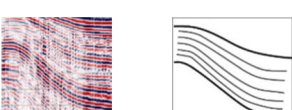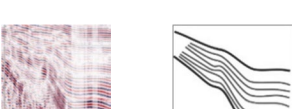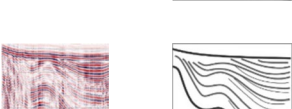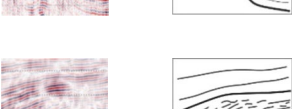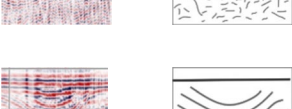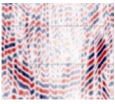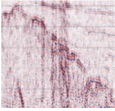
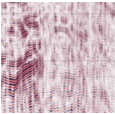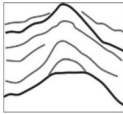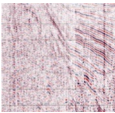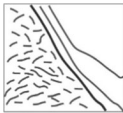| Facies types	Facies presentation	Reflection features	Geological interpretation
SF-1		*Shape*: sheet; *Texture*: parallel to subparallel; *Features*: high amplitude, continuous, high frequency	Low energy environment related to lake-floor or basin-floor deposits
SF-2		*Shape*: sheet-drape; *Texture*: wavy parallel; *Features*: high-to-low amplitude, continuous, high frequency	Compressional folding associated with fine-grained deposition
SF-3		*Shape*: wedge; *Texture*: oblique parallel; *Features*: moderate amplitude, semi-continuous, high frequency	High energy environment with better sorting of coarse-grained deposits in channels & bars
SF-4		*Shape*: wedge; *Texture*: oblique tangential; *Features*: moderate-to-low amplitude, semicontinuous, moderate frequency	Excessive sediment supply, high energy, coarse-grained delta deposits with poor sorting & shows sea-level standstill
SF-5		*Shape*: wedge; *Texture*: oblique sigmoidal; *Features*: moderate-to-low amplitude, semicontinuous, moderate frequency	Moderate sediment supplies with high sea-level, fine-grained low energy deposition by prograding slope & poor sorting
SF-6		*Shape*: local-chaotic; *Texture*: chaotic; *Features*: moderate-to-low amplitude, low-continuity, low frequency	Triggered by earthquake, & represents slump deposits
SF-7		*Shape*: chaotic; *Texture*: chaotic; *Features*: low amplitude, low-continuity, high frequency	Basement deposits
SF-8		*Shape*: divergent-fill lens-shaped; *Texture*: onlap & wavy parallel; *Features*: moderate amplitude, continuous, high frequency	Generally, shale-prone low-energy sediments, shows later stages of graben fill
SF-9		*Shape*: onlap-fill lens-shaped; *Texture*: onlap & lens; *Features*: moderate-to-low amplitude, low continuity, low frequency	Generally, low-energy filling of erosional channel
SF-10		*Shape*: complex-fill lens-shaped; *Texture*: onlap & downlap; *Features*: moderate amplitude, semi continuous, moderate frequency	High variations in sediment provenance and water flow

Table 3 (continued)

Facies types	Facies presentation	Reflection features	Geological interpretation
SF-11		*Shape*: chaotic-fill lens-shaped; *Texture*: chaotic; *Features*: moderate-to-low amplitude, low-continuity, low frequency	High-energy fill
SF-12		*Shape*: mound; *Texture*: onlap, velocity sag; *Features*: low amplitude, low-continuity, low frequency	Carbonate-prone deposits in shelf-edge settings
SF-13		*Shape*: mound; *Texture*: velocity pull-up; *Features*: low amplitude, semi continuity, low frequency	Carbonate-prone deposits having multi-stage growth
SF-14		*Shape*: slope-front fill; *Texture*: parallel divergent; *Features*: high amplitude, continuous, low frequency	Deep water deposits such as fans, and shows clays & silts in a low-energy environment

Fan facies are recognized by downdip reflections that are internally chaotic and wedge-shaped with planar basal surfaces (Soreghan et al. 1999). They usually comprise coarser mass-flow packages with low internal grading (Wells et al. 1999). These facies include slope fan facies, canyon fan facies, and delta-fan facies (Fig. 2c).

Channel-fill facies have U-shaped and convex bottom features on seismic sections (Anees et al. 2019) and are usually composed of medium-amplitude and medium-frequency reflections that might truncate adjacent to each other (Lyons et al. 2011). Channels are also characterized by fining-upward sequences and coarser gravity flow packages (Wells et al. 1999). Levees are often linked with channels, display a topographically higher location with respect to the channels, and exhibit high amplitude and transparent seismic features (Torrado et al. 2020) (Fig. 2d).

Basin-fill facies are associated with the depocenters of the basins and are composed of semicontinuous, high-frequency, and low- to high-amplitude internal reflections. Externally, these patterns are basal onlapping patterns (Wells et al. 1999) (Fig. 2e).

4.2 Seismic sequence stratigraphic analysis

We have presented a comprehensive analysis of the acquired seismic profile of each survey line in the Lake Fuxian basin. To analyze the depositional sequences, we subdivided the seismic reflections into a set of packages with identical external geometry (shape) and internal geometry (features and texture) that can be distinguished via sequence boundaries. Overall, we analyzed 14 different seismic facies types (SFs) and presented an abridged form of graphical presentation, shape, texture and reflection features, as well as their geological significance and interpretation, in Table 3. Initially, the seismic packages of depositional sequences were marked on the L6 dip line, which is the main survey line and represents the whole structural and stratigraphic setting of the lake basin (Fig. 3). Later, the depositional sequences were marked at the intersection of each survey line based on the regional geology and the corresponding reflection sequences. It is preliminarily inferred that the effective reflection sequences of the main chronostratigraphic interface can be divided into 6 horizons and 5 sequences. These horizons are marked as T_0, with T_1, T_2, T_3, T_4, and T_g (youngest to oldest).
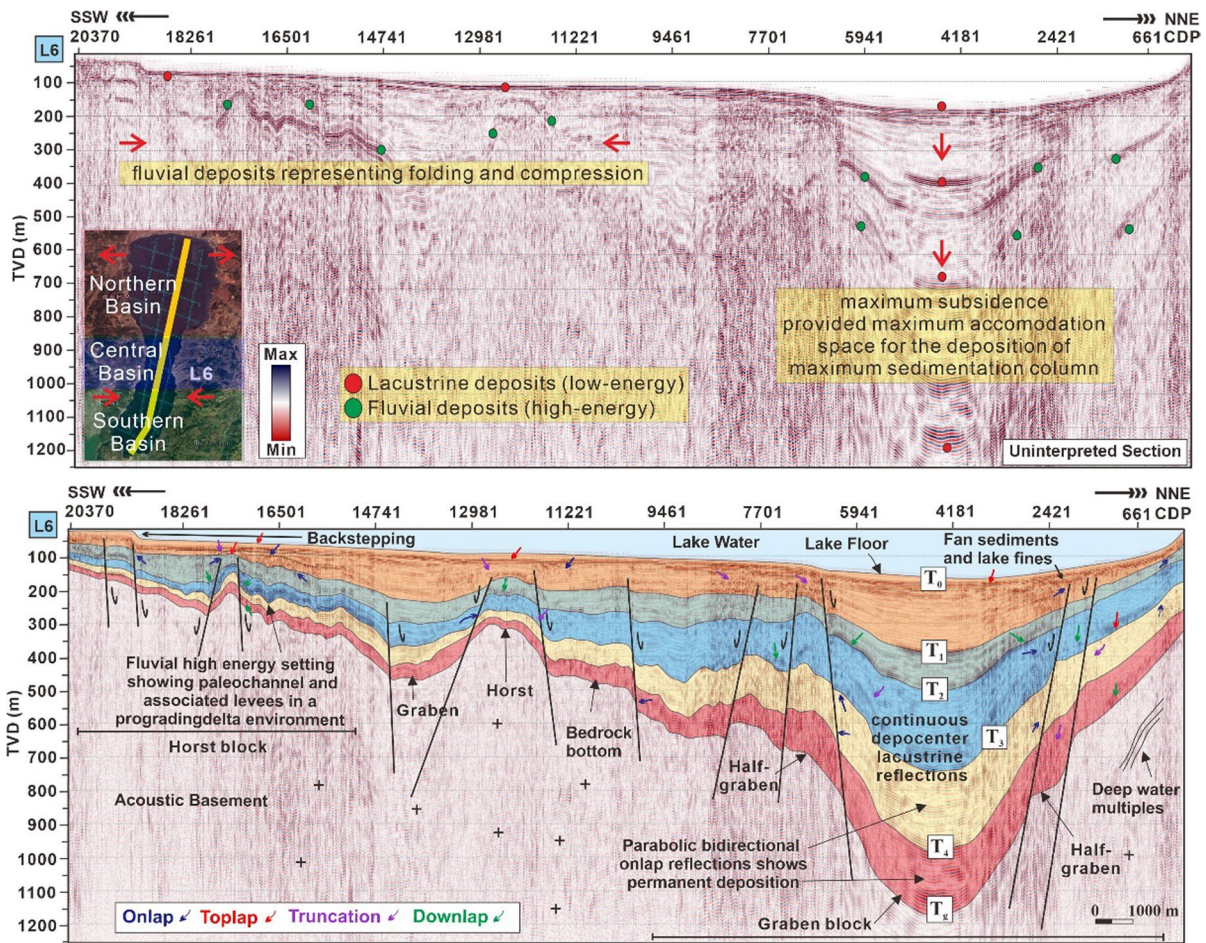
Fig. 3 Uninterpreted (top) and interpreted (bottom) seismic sections showing stratigraphic sequences and associated variations in the L6 dip survey line

4.2.1 Sequence-1 (Sq-1)

The topmost depositional package in the research region is Sq-1, which lies between the T_0 and T_1 horizons. The present-day sediment–water contact is near the top of Sq-1, which is marked by the T_0 horizon. The deepest point of the T_0 horizon is 171 m, which lies at the L10-2 survey line (Fig. 4). The thickness of Sq-1 varies from 16 m in the SSW region to 501 m in the NNE region. The maximum thickness of Sq-1 is 330 m, which lies at the L10-2 survey line near the NW region. The minimum thickness is 39 m, which lies toward the SSW region of the lake near the L1 survey line.

The seismic texture in Sq-1 shows parallel and wavy reflections in the middle and discontinuous reflections toward the margin that depict sheet-drape geometry. These reflections are related to the uniform deposition of silt and clays along with organic matter in the Holocene sediments. The parallel reflections at the top are marked by a toplap, whereas the down-dipping reflections are mapped through the demarcation of onlaps and downlap patterns toward the NEE region of the basin, where the topography of the Lake Fuxian basin changes from a homoclinal ramp to distally steeper slope ramps (Fig. 3). The reflections of Sq-1 gradually terminate on tilted Sq-2 reflections, creating an unconformable contact at the L6 survey line near the 17,150 CDP.
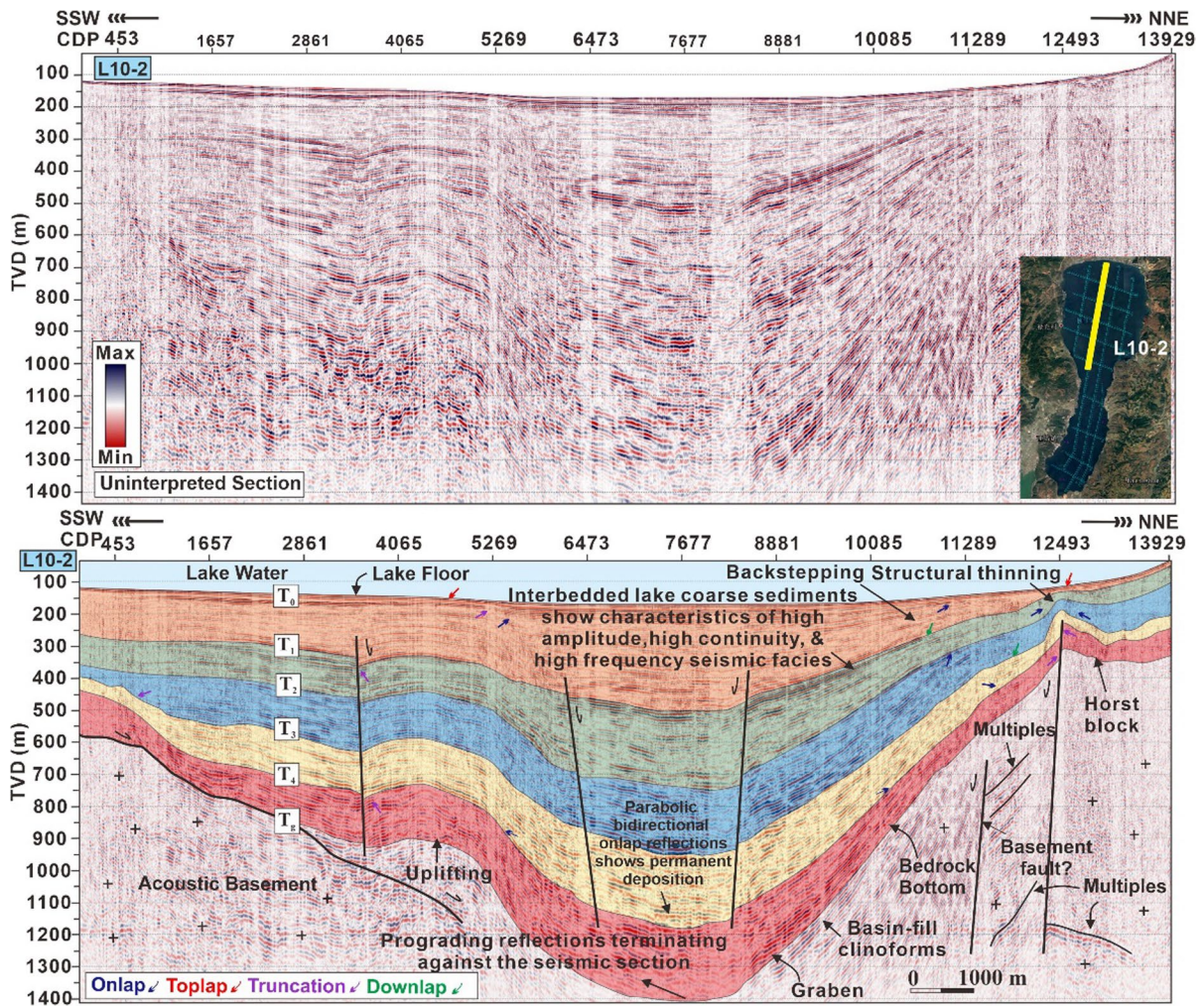
Fig. 4 Uninterpreted (top) and interpreted (bottom) seismic sections of the L10-2 survey line showing the northern lake basin

Sq-1 is mostly characterized by high-amplitude, high-frequency, and parallel to subparallel continuous seismic reflections (SF-1). These facies are associated with the low-energy environment of lake-floor deposits. In contrast, toward the depocenter region, the reflections exhibit the characteristics of high-to-low amplitude, high frequency, and wavy parallel reflections (SF-2), which extend to a few kilometers. These facies are related to the folding of the strata and feature fine-grained deposition. The two types of facies that are dominant in Sq-1 are hemipelagic drape facies and channel-fill facies. The reflections of hemipelagic drape facies exhibit very low amplitudes and onlap to the existing reflections on the lake floor (T_0) (Fig. 2a). However, the channel-fill facies in Sq-1

are mainly characterized by divergent-fill (SF-8) and complex-fill (SF-10) facies. The onlap pattern of the divergent-fill facies shows low-energy, shale-prone sediments in the graben-fill. However, the complex filling of the channel provides an indication of rapid variations in water and sediment provenance. In a general trend, the uppermost reflections of the channel-fill facies truncate onto the preexisting reflections of Sq-1.

4.2.2 Sequence 2 (Sq-2)

Sq-2 is situated beneath Sq-1 and lies amid the T_1 and T_2 horizons. Sq-2 cannot be tracked throughout the lake basin, and some reflections terminate on the
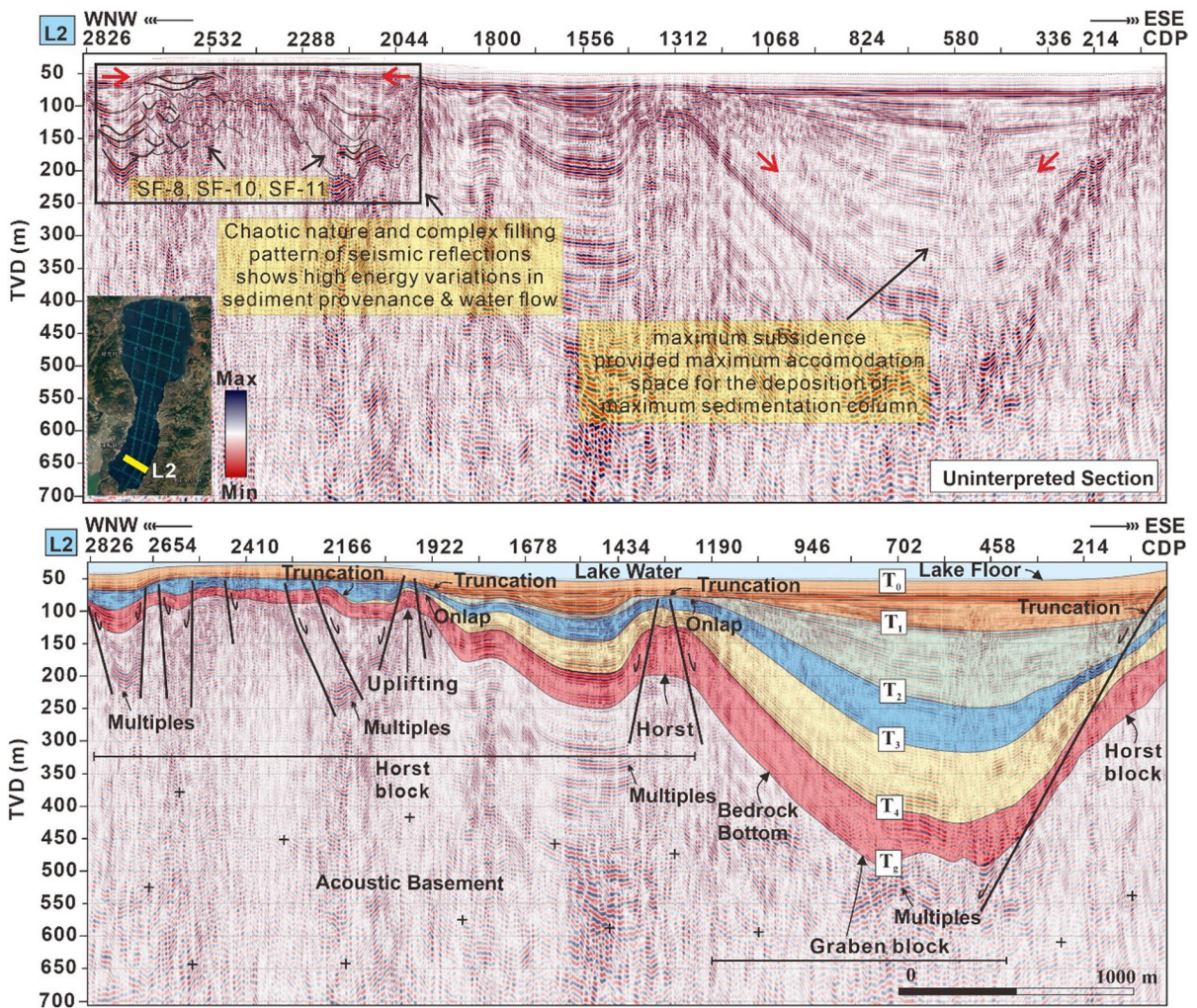
Fig. 5 Uninterpreted (top) and interpreted (bottom) seismic sections of the L2 survey line showing the southern lake basin. The interpreted section shows lake sequences associated with seismic variations

reflection pattern of Sq-1. This termination is evident at the L2 survey line near 1922 and the 1312 CDP (Fig. 5). The structural thinning of stratigraphic Sq-2 is also evident at L10-2 toward 12,493 CDP (Fig. 4). Sq-2 is thinner than Sq-1. The maximum thickness of Sq-2 is 187 m, which lies at the L10-2 survey line near the NW region toward the depocenter of the basin. The minimum thickness of Sq-2 lies at L2, where the reflections terminate against the overlying gently dipping strata of Sq-1.

Within Sq-2, the parallel reflections of overlaying strata of Sq-1 are marked by toplap, whereas the downdipping prograding packages are traced via onlaps and downlapping patterns toward the SSW

and NNE regions of the basin. The basal contact of Sq-2 displays high-angle reflections toward the margin of the seismic sections and shows wedge-shaped prograding fan facies reflections (Fig. 2b). These fan facies are semicontinuous and feature oblique tangential and sigmoidal texture textures (SF-4 and SF-5). However, the reflections are flat-layered but wavy in the middle region and show sheet-drape geometry (SF-2).

Further toward the NNE region of the lake basin, the reflections of Sq-2 change the morphology from wavy parallel to oblique parallel reflections, where the topography of the basin changes from sheet-drape (SF-2) to a distally prograding fan facies. These
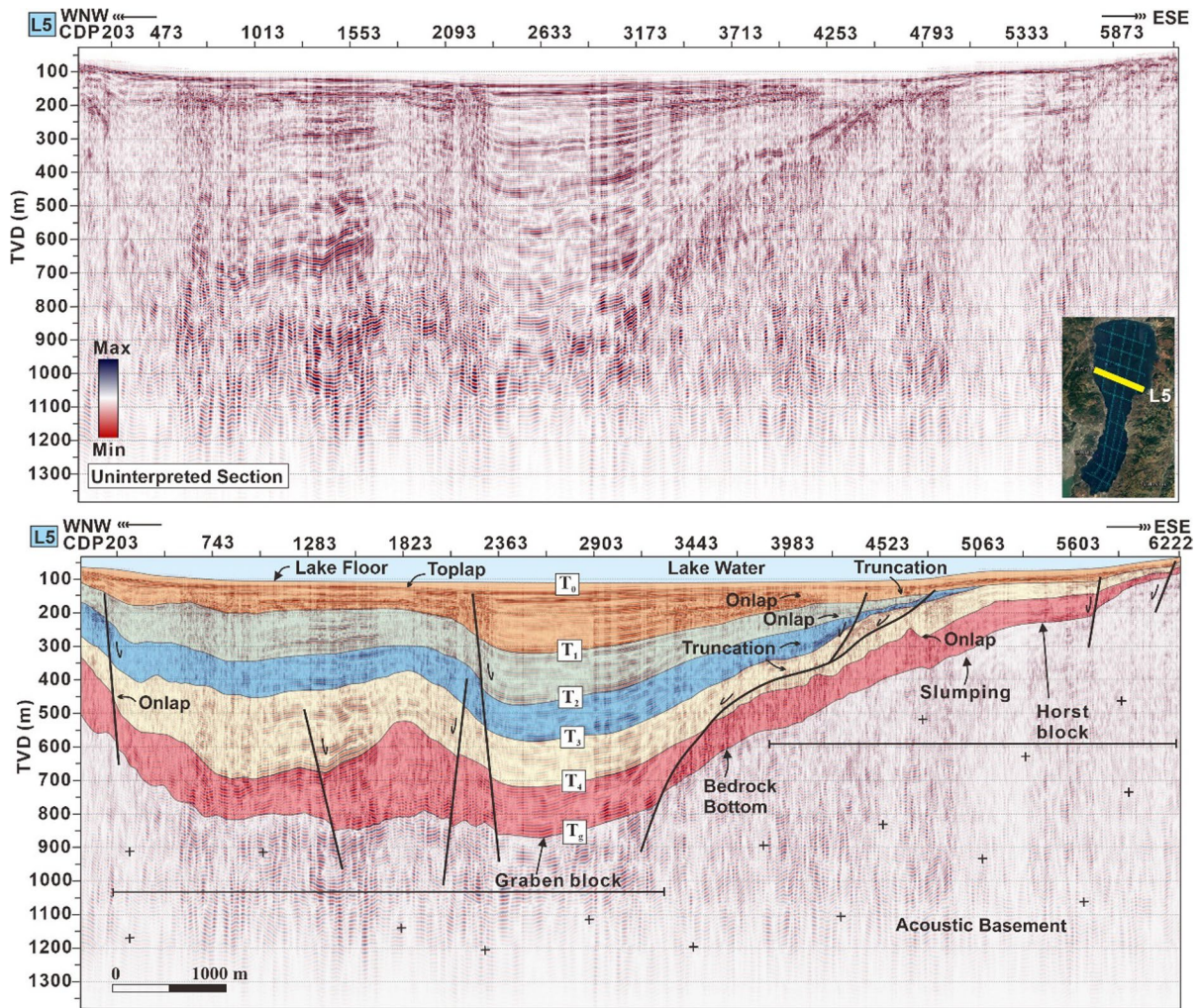
Fig. 6 Uninterpreted (top) and interpreted (bottom) seismic sections of the L5 survey line showcase the presentation of the central lake basin. The interpreted section shows the interpretation of the lake sequences associated with seismic variations

fan-shaped facies are associated with high-energy interbedded lake coarse-grained facies that are associated with sand and gravel, whereas the subparallel to wavy reflections within Sq-2 are associated with intercalations of silt and clays. The existence of irregular diffracted reflections is possibly associated with paleosemic activity during the Holocene.

4.2.3 Sequence 3 (Sq-3)

Sq-3 lies beneath Sq-2 between the T_2 and T_3 horizons. The reflections of Sq-3 terminate against the Sq-2 reflections. In some cases, Sq-3 reflections

terminate against Sq-1 reflections, forming an unconformable contact. Hence, the reflections of Sq-3 cannot be tracked throughout the lake basin. These terminations on Sq-1 are evident at the L5 survey line near the 5063 CDP (Fig. 6). Sq-3 is thicker than Sq-2. The maximum thickness of Sq-3 is 272 m, which lies at the depocenter of the L10-2 survey line. Structural thinning of Sq-3 is evident toward the SSW region of the lake basin (Fig. 5). The minimum thickness of Sq-3 is 6 m, which is observed at the L2 survey line near the 1922 CDP. The basal contact of Sq-3 shows high-angle reflections terminated against the Sq-2 and Sq-1 horizons. The reflection characteristics of Sq-3

are highly variable. At several locations, the semi-continuous reflections of Sq-2 and Sq-3 form convex-bottom features and establish local unconformities via erosional truncations of the overlaying sequence reflections.

Toward the SSW region of the lake basin, there are numerous high-amplitude parabolic-shaped reflection patterns (Fig. 2d). These parabolic reflections formed the horst block toward the southern region of the lake basin. The convex-bottom features show the characteristics of lens-shaped, high-amplitude, semi-continuous, low-frequency and high-angle reflections on the seismic section and are associated with channels. The adjacent linked wedge-shaped, uplifted, and high-amplitude features show levees. The sediments associated with these parabolic features are coarse-grained in the channels and are overlain by fine-grained facies in the levees.

Sq-3 shows the characteristics of prograding clinoforms associated with SF-3 and Sf-4, as evident at the middle of the L5 strike line and L6 dip lines. Toward the NNE region of the lake basin, Sq-3 features slope-front deposits (SF-14), which are linked with foreset and bottomset beds (Fig. 5). These high-dipping reflections are characterized by onlaps and downlap patterns and exhibit low-amplitude, continuous, and high-frequency features. The morphology of the clinoforms varies among SF-3, SF-4 and SF-5. However, steeply dipping foresets are always terminate at the top of sequence-4.

The lenticular-shaped channel-fill facies present in Sq-1 have a deep impact on the lake sediments. The effects of these channel-fill facies are prominent within Sq-2 and Sq-3 and extend to the deeper sequences of the Lake Fuxian basin (Fig. 7a). These channel-fill facies are associated with coarse-grained sand and shale sediments.

4.2.4 Sequence 4 (Sq-4)

Sq-4 is located under Sq-3 between the T_3 and T_4 horizons. The reflections of Sq-4 terminate against the Sq-3 reflections. As a result, toward the margins of the lake basin, Sq-4 reflections cannot be traced across the whole lake basin at some survey points. These terminations may be observed near 2166 CDP

Fig. 7 **a** Presentation of different types of channel-fill facies toward the southern basin showing variations in sediment provenance and water flow. **b** Slumping and complex filling seismic reflections providing indications of paleosemic activity that occurred during the Cenozoic era. **c** Mound-shaped deposits associated with carbonate buildups. **d** Evidence of backstepping of the progradational delta toward the central basin of the lake. **e** Aggrading and prograding fans indicating highstand settings. **f** Clinoforms terminating against the seismic section toward the northern basin of Lake Fuxian, indicating the deepest and oldest permanent sedimentation
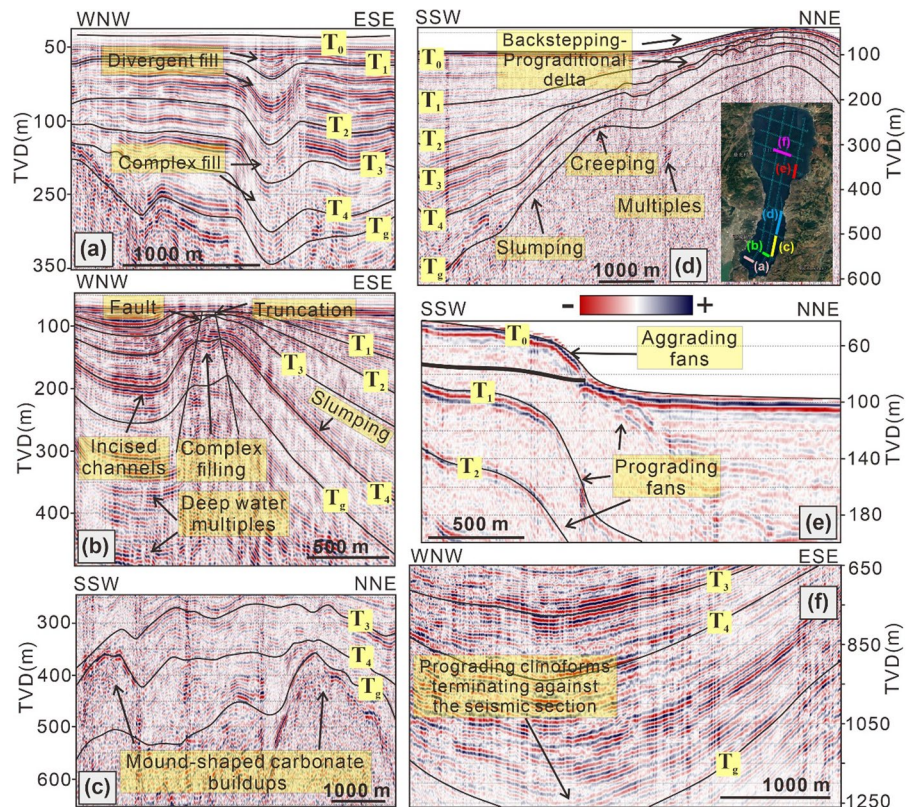
on the L2 survey line (Fig. 5). The thickness of Sq-4 is highly variable. The maximum thickness of Sq-4 is 247 m at L10-2, which is less than the 272 m thickness of Sq3 at the same location. The thickness of Sq-4 is also lower at the L6 survey line. However, the thickness of Sq-4 is greater than that of Sq-3 at some locations on the L2 and L5 survey lines.

The reflections of Sq-4 have a wide range of features. The basal contact of Sq-4 features steeply dipping reflections, and the external geometry is mainly characterized mainly by mound-shaped and wedge-shaped facies. Toward the SSW region of the lake basin, there is a mound-shaped concave feature where reflections of Sq-3 are gently dipping and onlapping onto the mound-shaped reflections of Sq-4. This feature is evident on the L5 survey line near the 1823 CDP and was termed SF-12 in our study (Fig. 6). This texture was associated with velocity sag and is usually associated with carbonate-prone deposits in shelf-edge settings (Schlaf et al. 2005). The internal geometry of these reflections shows low amplitude, low continuity, and low frequency.

Numerous stacked oblique tangential (SF-4) and sigmoidal (SF-5) clinoforms also tend to appear within Sq-4 toward the northern basin of the lake. The depositional sequence is marked by a succession of well-built, northeast-trending prograding clinoforms toward the graben-fill distal region. Lens-shaped features also occur within Sq-4 that lie toward the WNW region of the lake basin and are associated with complex fill (SF-10) and chaotic-fill channel-shaped geometry (SF-11) (Fig. 7b). The internal texture of the reflections is chaotic and is associated with high-energy and rapid filling of sediments. These facies are the deeper versions of SF-8 at the L2 survey line, as described in the Sq-2 explanation (Fig. 7a).

At the center of the lake, there are some mound-shaped reflections that thicken the seismic structure. These mound features are associated with backstepping of the prograding delta facies (Fig. 7d, e) and represent flooding surfaces that are associated with retrogradation of the lake.

4.2.5 Sequence 5 (Sq-5)

Sq-5 is the oldest depositional sequence in the basin that can be tracked in the study area. Sq-5 is situated beneath Sq-4 and lies between the T_4 and T_g horizons. The T_g horizon marks the top surface of the basement. There are continuous frequent irregular chaotic facies, which confirms the presence of basement below the T_g horizon. The reflections of Sq-5 can be tracked throughout the basin at every survey line. The thickness of Sq-5 is variable. The maximum possible thicknesses are 206 m at L10-2 and 310 m at the L8 survey line, toward the depocenter of the basin where there is a prominent graben structure at the regional level, creating additional accommodation for the lake sediments. At the L10-2 survey line, the reflections of Sq-5 show the internal geometry of moderate reflections and semicontinuous and high-frequency features and prograde until the end of the seismic sections, which indicates that the thicknesses of Sq-5 can further extend to ~50 m until the start of the basement (Fig. 7f).

The reflections of Sq-5 terminate and overlap with the reflections of Sq-4. This depositional sequence features a variety of facies patterns. The basal contact of the Sq-5 reflections is marked by downlap features. The reflections of Sq-5 show a V-shaped onlap-fill lenticular external geometry. The internal geometry of the reflections is characterized by moderate-to-low amplitude, low continuity, and low frequency (SF-9). The geological significance of SF-9 is interpreted as the low-energy filling of erosional channels. Sq-5 also shows local-chaotic reflections. The internal geometry of these reflections is chaotic and characterized by moderate-to-low amplitude, low continuity, and low frequency (SF-6). These chaotic reflections are sandwiched amid the smoothed oblique parallel reflections, which are possibly caused by paleoseismic activity and denote slump deposits.

Sq-5 shows frequent mound-shaped features that are evident at the L2 (1312 CDP) and L5 (1823 CDP) survey lines. These reflections are concave-shaped and are named SF-13 in our study. The external geometry is mound shaped, the texture is termed velocity pull-up, and the internal features exhibit low amplitude, semicontinuity, and low frequency. These mound-shaped facies are also prominent toward the SE region of the basin (Fig. 7c). The cause of the difference in the SF-13 facies is the combination of the high-velocity zone in Sq-4 against the low-velocity zone in Sq-5 (Trinchero 2000). These facies are associated with carbonate-prone deposits with multistage growth (Schlaf et al. 2005).

The wedge-shaped reflections within Sq-5 show a slope-front fill geometry with high-angle dipping parallel divergent reflections, and the internal features show high amplitude, continuity, and low frequency (SF-14). These reflections are linked with deep water fan facies and show clays and silts in a low-energy environment (Fig. 7d). These facies are also evident in the ESE region of the L2 survey line. The sheet-shaped reflections within Sq-5 are parallel to subparallel shapes and show high amplitude, high continuity, and high frequency. These reflections are characterized as basin-fill facies and are linked with a low-energy environment related to basin-floor deposits. There are thick-bedded basin-fill lacustrine facies at the depocenter of the lake basin, and the reflections show bidirectional onlap patterns that indicate the permanent and oldest sedimentation of the lowstand settings (Fig. 4).

4.2.6 Basement

Below Sq-5, there is a frequent presence of chaotic texture, which is associated with the basement (SF-7). The topmost part of the acoustic basement features the characteristics of frequent discontinuous reflections establishing a main unconformity toward the base of the sedimentary layer. The external geometry is irregular, with low coherence and no specific characteristics. However, the internal features show low amplitude and low continuity. These features confirm the presence of basement material. These poorly established reflections are probably associated with the Moho discontinuity because of poor-quality seismic responses in the deeper regions of the seismic sections. Several deep water multiples and diffraction patterns are also observed in the acoustic basement region.

5 Discussion

5.1 Evidence of lake-level variations by drilling cores from Sq-1

Several contemporary studies conducted on the Lake Fuxian basin have utilized drilling cores within the lake epilimnion zone (~3 m deep on the lake floor) to evaluate the effects of paleoclimate and grain-size characteristics (Wang et al. 2018; Li et al. 2019a, b; Yin et al. 2021; Wang et al. 2021a, b). The deepest core drilled in the study area has a length of 900 cm and is drilled toward the southern basin of the lake at a depth of 81.2 m (Sun et al. 2018). Their results showed that the maximum sediment accumulation rate was 2.3 mm/a. In another study, the authors used a core of 296 cm, which was situated in the southern basin near L3 (Li et al. 2019a, b). The authors used this core to examine variations in lake level over the previous ca. 12 ka. Their research revealed that the sedimentation rate of the 296 cm core was 0.24 mm/a. However, the average sedimentation rate of all seven drilled cores was 1.6 mm/a, which is lower than that of other lakes within the Yunnan Plateau (Wang et al. 2018) (Table 4). There could be several reasons for the lowest sediment accumulation rates within Lake Fuxian: (a) the deepest lake among all the other Yunnan Plateau lakes and a reasonably extended water exchange period (Barrpso et al. 2015), (b) the maximum water transparency in comparison with that of other lakes, and (c) the minimum turbidity (Wang et al. 2018). These are the main factors that contributed to the lowest sediment accumulation rates in Lake Fuxian.

The results of the other cores toward the deepest waters in the northern basin of Lake Fuxian show

Table 4 Average sedimentation accumulation rates (SARs) and transparencies of the Yunnan Plateau lakes in China

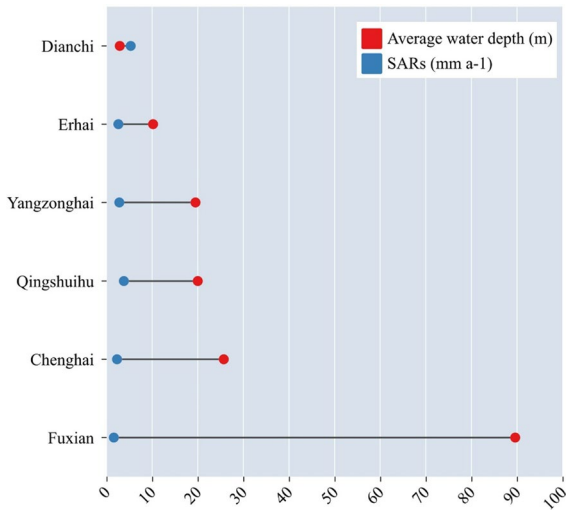| Lakes	Average water depth (m)	Core lengths (cm)	SARs (mm/a)	Transparency (m)	References
Dianchi	2.9	–	5.3	0.2–1.2	Liu et al. (2013b)
Erhai	10.2	35	2.6	2.0–6.5	Liu et al. (2014)
Yangzonghai	19.5	44	2.8	4.5	Zhang et al. (2012)
Qingshuihu	20.0	40	3.8	2.0	Liu et al. (2013a)
Chenghai	25.7	43	2.3	3.0–3.5	Liu et al. (2015)
Fuxian	89.6	23	1.6	7.0–8.0	Wang et al. (2018)

Fig. 8 Average water depths and SARs of various Yunnan Plateau lakes

the presence of fine sediments eroded from various tributaries in the northern catchment in steady and relatively weak hydrodynamic settings (Wang et al. 2018). Fine sediments are mainly composed of organic matter, silt and clay (Yin et al. 2021). However, toward the middle and southern regions of the lake basin, coarse-grained sediments were observed in the shallow water due to the presence of strong hydrodynamic conditions (Wang et al. 2021a, b). The coarser grain size in the middle of the lake could be related to complicated hydrodynamic conditions because of the nearby outlet of the lake basin (Wang et al. 2018). However, toward the southern basin of the lake, carbonates are quite abundant. Carbonates are mostly composed of calcite, and Ca is present in ample amounts in carbonates compared to other minerals (Li et al. 2019a, b).

However, the accuracy of evaluating of these sedimentation rates in the deeper regions of the stratigraphic succession, other than Sq-1, cannot be justified due to the absence of drilling cores. The SARs and average water depths of the various Yunnan Plateau lakes are shown in Fig. 8.

5.2 Effect of seismicity on the paleoseismic events

Lake Fuxian is a tectonic lake located on the XJF. The seismicity of the XJF is quite strong, and approximately ten robust earthquakes with magnitudes M > 6

have occurred along the Xiaojiang seismic belt (Wang et al. 2009). Therefore, the sedimentation of the Lake Fuxian basin and other nearby regions of eastern Yunnan was affected by these tectonic activities. Seismic activity results in landslides and destruction of surface vegetation. Lake seismic waves trigger the surface to tremility, causing disruption of the loose sedimentation in the lakebed sediments (Fig. 7b).

Recently, many authors have conducted research on paleoseismic records of lacustrine sediments (Lyons et al. 2011; Dietze et al. 2012; Jiang et al. 2017; Wang et al. 2021a, b). The identification of paleoseismic events through lacustrine sediments is more reliable and continuous than the conventional paleoearthquake evaluation technique (Wang et al. 2021a, b). The grain-size analyses better reveal the lacustrine events associated with paleoearthquakes. In a recent study, the authors employed grain-size analyses within Lake Fuxian, which showed that unconsolidated lacustrine sediments are mostly composed of silt and clay (Yin et al. 2021). However, in another study of Lake Fuxian, the authors described that the lacustrine sediments are deformed and are affected by strong tectonic activity (Li et al. 2019a, b), which is also evident in our study (Fig. 5). These changes, in turn, have also disturbed the medium- to coarse-grained sediments, which subsequently underwent suspension and redeposition. The coarse sediments were deposited faster due to high energy generated by gravity, while the fine sediments in suspension subsequently accumulated (SF-6 and SF-11).

5.3 Assessment of lake-level variations through seismic stratigraphy

The depositional sequences established for the Lake Fuxian basin provide useful insight into the relative chronology for interpreting the paleodepositional architecture. The sequences marked and their relationships with the lake-level variations are as follows:

Sq-5 and Sq-4 represent the deposition of the lake basin at a low lake level. Sq-5 is interpreted as the deposition of sediments during the late lowstand tract (LST), while Sq-4 shows sedimentation during the early LST. The presence of clinoforms, along with a significant angular conformity in the updip direction, shows the prominent signs of lowstand environments during this period (Figs. 3, 7f). The coastline of the lake migrated ~ 1.5 km toward either side horizontally

during the evolution of these clinoforms in the southern basin when these clinoforms evolved (Fig. 5). The situation toward the middle basin is almost the same, and ~2 km of horizontal migration toward the ESE region is evident (Fig. 6). However, toward the northern region of the Lake Fuxian basin, the coastline migrated ~4 km to the NNE and ~19 km to the SSW of its present position (Fig. 3). The clinoforms in the northern region of the basin covered extra space toward flexural margins due to the presence of half-graben and graben structures (Fig. 4). The developed clinoforms within the extensional regimes are generally linked with a flexural margin river region (Scholz 1995). Therefore, the flexural marginal clinoforms in Sq-4 and Sq-5 are interpreted as prograding low system tract (LST) delta deposits. Similar lowstand delta deposits in extensional regimes were also revealed by the authors in their studies of Lake Edward and Lake Malawi (McGlue et al. 2006). The clinoforms are piled in such a way that the oldest prograding layers are evident in the bottommost stratal region. Due to the presence of normal faults, the stratigraphic structure of the lake basin has a low gradient. These low-relief clinoforms are associated with the graben block (Fig. 3). Therefore, it is inferred that the lake level during deposition of Sq-5 was ~930 m beneath the up-to-date lake floor.

Mound-shaped deposits are evident within these two sequences (SF-12 and SF-13). These deposits are possibly associated with carbonate deposits. The carbonate in the sediments of Lake Fuxian is mainly composed of calcite (especially Ca) (Li et al. 2019a, b). The frequent presence of these mound-shaped deposits is associated with a higher content of carbonates ($CaCO_3$), which reflects a decrease in the lake water level, a decrease in lake surfaces, and an increase in drought duration (Menking et al. 1997; Li et al. 2019a, b). During drought conditions, the lake area was dry with little rain due to the arid environment, surface runoff was low, and the physical transport function of the lake area was quite weak. Due to these conditions, insoluble minerals in the rocks, such as quartz, feldspar and clay minerals, had difficulty migrating to the lake in mechanical physical form. However, soluble minerals such as calcite migrate into the lake basins in ionic or colloidal states through surface water and groundwater through chemical erosion. During the lake shrinkage environment and strong evaporation, the carbonates precipitated or were possibly absorbed to the bottom of the lake in Sq-4 and Sq-5. The presence of slope-front fill strata within Sq5 suggested the deposition of deep water fans associated with fine-grained sediments such as clay and silt in a low-energy environment (SF-14). Toward the southern basin, these low-energy deposits are associated with V-shaped onlap-fill erosional channels (SF-9). The presence of SF-6 within Sq-5 provides evidence of slump deposits, which suggests that these deposits were triggered by earthquakes since the Lake Fuxian basin existed in the active tectonic region due to the presence of the XJF (Wang et al. 2009).

Sq-3 and Sq-2 are interpreted as deposited during an overall retrogrational period. Sq-3 is interpreted as the deposition of sediments during the early transgressive stages in the lake basin after the major regressive stages in Sq-4 and Sq-5. However, Sq-2 shows deposition during the late stages of the highstand settings. Overall, these two sequences show the characteristics of medium- to low-amplitude, high-continuity and high-frequency reflections, suggesting a different paleoenvironment than the deeper sequences of lowstand packages. Several wedge-shaped (SF-5) and parabolic-shaped patterns (SF-2 and SF-10) are evident in the seismic section within Sq-3. These reflections are situated updip of the Sq-4 clinoform and indicate a retrogradational deltaic pattern. In the literature, transgressive deltaic sedimentation has been documented in marine shelf settings (Porębski and Steel 2006). Therefore, we inferred that the strata of Sq-3 were deposited during retrogradation in proximate coastline settings. These reflections are evident and are marked by several episodes of onlapping patterns (Fig. 7d, 7e), which denote the backstepping prograding delta deposits. The wedge-shaped reflections indicate a moderate sediment supply and are associated with a rise in sea level, where fine-grained low-energy sediments were deposited by pooly sorted prograding slopes with poor sorting (Fig. 7b). The parabolic-shaped reflections indicate the presence of a high-energy fluvial environment in the form of channels and levees (Fig. 7d). The textures of these channel-filled reflections are onlap and indicate the presence of shale and sand deposition. The sedimentary thickness of the lake is highly variable in the middle and northern regions compared to that in the southern region. The sedimentation of Lake Fuxian was affected by tectonic activity (Li

et al. 2019a, b), and reflections are missing in some zones, which could be related to the absence of sedimentation in some parts (Fig. 7c).

Sq-1 is interpreted as the preliminary stage of hemipelagic deposition in a profundal paleoenvironment. The hemipelagic drape facies shows the characteristics of continuous parallel seismic reflections that establish a prominent onlapping pattern with the preexisting reflections from the lake floor (Fig. 7a). Overall, these seismic reflections of Sq-1 are composed of parallel to subparallel, divergent and semicontinuous reflections, distinguishing them from the underlying seismic reflections that are representative of relatively deep waters of the Lake Fuxian basin. The drilled cores within Sq-1 suggest the presence of ooze, detrital clay, silt and intercalated of organic matter that was accumulated by suspension (Wang et al. 2018). The presence of these fine-grained sediments also indicates that sedimentation was controlled by suspension. Continuous straight reflections are present at the regional level throughout the basin within Sq-1, suggesting that prevalent deepwater settings occurred during most of the Sq-1 timescale. However, in a recent study, the authors suggested that the last rise in the lake level occurred at ~2.2 cal. Ka B. P and reached the modern lake surface (Li et al. 2019a, b).

5.4 Geological controlling factors influencing sedimentation in lake basins

Tectonic lakes often form as a consequence of rifting and strike-slip tectonics occurring in an extensional environment (Sladen 2012). Climate change has a greater and more lasting impact on the hydrology of rift-lake basins compared to basin geodynamics or volcanism, when considering shorter periods of geologic time within the African rift lakes (McGlue et al. 2008). Some of the main factors that play a crucial roles in controlling the evolution of great global lake sequences include analyzing the subsidence rate versus the accumulation rate, climate, sedimentary thickness, and geology of the rock types (Bohacs et al. 2000; Gierlowski-Kordesch and Kelts 2000; Sladen 2012). In another study conducted on the lake Malawi, the authors suggested that sediment supply and lake-level variations are relatively important factors in controlling lake sequences (Lyons et al. 2011).

In addition, the slope curvature of the clinoforms also provided important information about the in lakes Switzerland (Adams et al. 2001).

Tectonic forces have had a profound impact on lake deposits in the Fuxian Basin, molding the climatic and geological features of successive lake sequences. The results of seismic patterns toward the southern edge of L3 show circular-shaped low amplitude chaotic reflections, providing evidence of intense seismic activity (Fig. 9a). In addition, a steep slope of around ~500 m transported the sediments to the deepest region under the influence of gravity triggered by strong tectonic influence. The chaotic reflections below the basement indicate a pretectonic regime. Above these reflections, subparallel low-energy lacustrine patterns are present that were deposited in the posttectonic regime. On the shallow surface, there are smooth seismic patterns occur, providing a evidence of stable tectonic regime. Toward the western side (WNW) of the southern basin on L2, the dominance of the SF-8, SF10, and SF-11 seismic facies provides sufficient evidence of folding and compression led by intense seismic activity (Fig. 5).

Three seismic survey lines L1, L2, and L3 extending WNW-ESE, are present in the southern lake basin. L1 is present at the southern end and has the lowest sediment thickness, high fluctuations and low extension of faults. The precise total sedimentary thickness was calculated from the lake-floor horizon (T_0) to the bedrock horizon (T_g). L2 and L3 have the maximum sediment thickness in the southern basin; however, L3 has a sediment thickness of ~450 m, which is greater than that of L2 (Fig. 9c). L3 nearly follows L2, where fault subsidence affects the ESE area and reflections are steeper than those in the WNW region. The wavy nature of the reflections toward the southern basin at L6 suggested folding and compression, thus, reducing the area of the lake basin.

L4 is situated in the center of the basin, at the narrowest point with an orientation of WNW-ESE, and it has a width of approximately 2.5 km. The maximum sedimentary thickness on L4 is ~350 m (Fig. 9d), and maximum denudation likely occurred where less sediment was transported and deposited, thus reducing the sedimentation column. The seismic lines in the northern basin show smoother reflections with good continuity, high frequency, and low-to-medium amplitude. There are fewer
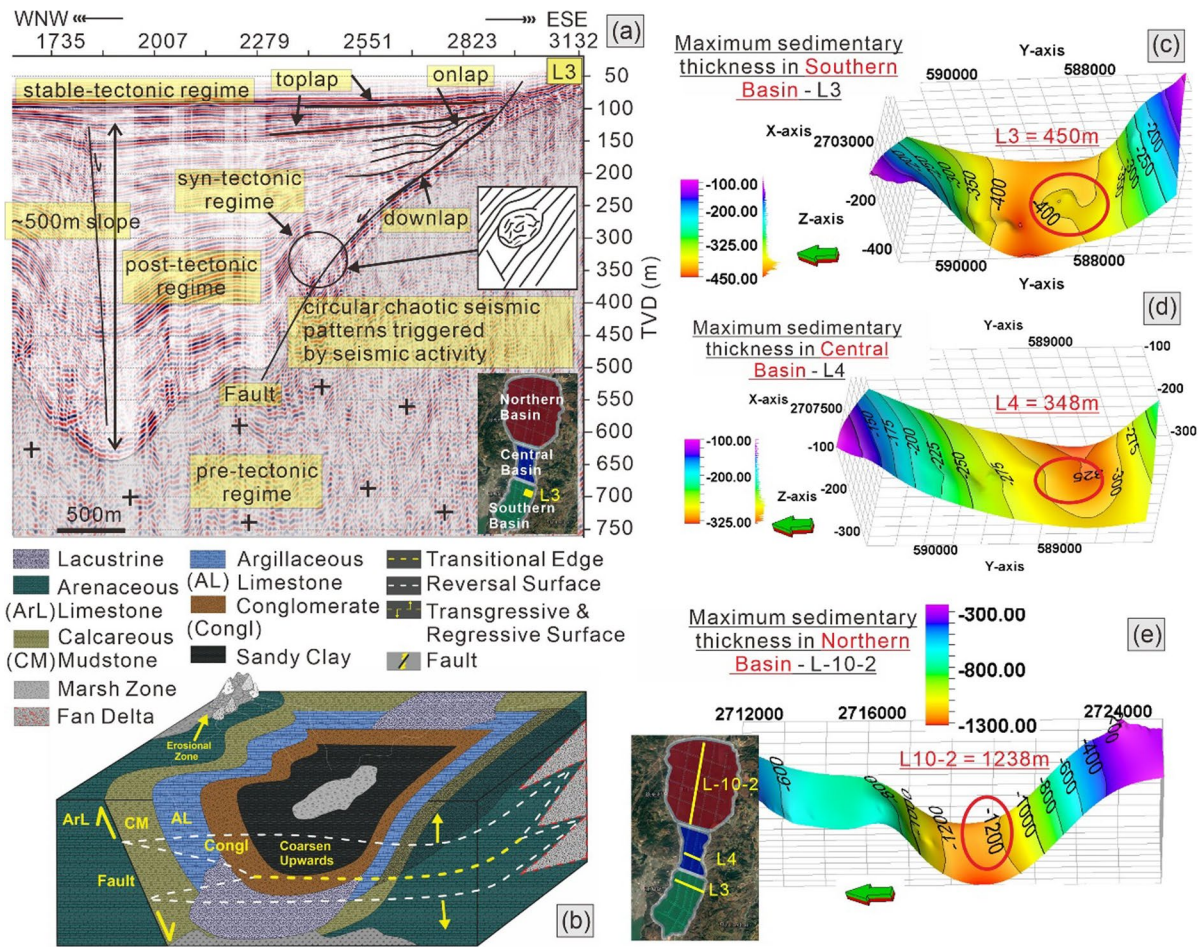
Fig. 9 a Seismic patterns on L3 representing events of tectonic regimes within the lake basin. **b** A proposed lake basin model showing generalized stratigraphy. **c**, **d**, and **e** Provide insights into the total sediment thickness distribution toward the southern, central and northern lake basins, respectively

fluctuations and the faults are steeper with a maximum throw. The maximum length of some of these normal faults extends beyond ~ 800 m, which strongly indicates that Lake Fuxian is a graben lake formed by fault subsidence with normal parallel faulting and an overall crustal extensional regime. The maximum subsidence in the northern basin provided the maximum space for sediment accumulation, thus, maximizing the sedimentation column (Fig. 3). The faults are parallel and show an extensional regime. Overall, the L10-2 has a maximum possible thickness of 1238 m and lies toward the NNW region in the Lake Fuxian basin (Fig. 9e).

In summary, the main controlling factor within the Lake Fuxian Basin is tectonics related to the normal faulting, which is the main cause of rifting and crustal extension and the formation of horst and graben structures. Other reasons include weathering and erosion (denudation), fill and subsidence, which contribute to the infilling of basin depressions, sediment accumulation rates (SAR), which are related to lake-level variations, sediment thickness distribution, and climate.

5.5 Depositional architecture of the Lake Fuxian basin

Tectonic lakes are responsible for the formation of some of the deepest and largest lakes in the world. These lakes are formed due to robust tectonic activities such as folding and faulting (Johnson 1984). Lake

Fuxian is also a tectonic lake on the Yunnan Plateau, and it is assumed that this lake formed due to tectonic activity during the late Pleistocene (Cui et al. 2008). Lake Fuxian is the deepest lake among the nine lakes within the Yunnan Plateau because tectonic activity has created crustal extension, and alternating series of horst and graben structures have formed. The results of the present study provide evidence that an extensional regime formed within the rift-lake basin formed due to fault subsidence. The lake basin comprises several parallel normal faults on both flexural margins of the lake (Figs. 2, 3). The structures that are dominant within Lake Fuxian are grabens, half-grabens, and horst structures. The source of the sediments was highlands, which were triggered by high seismic activity. Additionally, the clastic sediment depositional systems were considerably influenced by several geological events. Due to strong tectonic uplift, the western and eastern banks of Lake Fuxian are hilly, with steep slopes and extensive regions of reasonably dry ground (Dai et al. 2017). In addition, numerous karst landforms and limestone mountains have developed within the basin (Li et al. 2019a, b). Therefore, the sedimentation of the carbonates in the lake was quite abundant.

There are three main types of depositional landforms within the Lake Fuxian basin: lacustrine alluvial plains, alluvial fans and terraces. The Lake Fuxian basin is characterized by strong vertical movement, with fault block activity as a basic feature. Uplift and subsidence formed a vertical offset in adjacent blocks, resulting in terraces formation. The faults are also evident in these small blocks, giving rise to half-grabens. The regular parallel spacing contours on the bathymetry map (Fig. 1c) show the presence of a vertical offset that creates a trough-shaped basin termed the graben block in our study.

Several U-shaped and V-shaped erosional structures are also evident within the lake basin. These structures were properly described and named SF-8, SF-9, SF-10, and SF11 in our study. These features reveal the presence of channels that are associated with variations in sediment provenance and water flow. The main lithologies associated with these features are sand and shales. However, the mound features named SF-12 and SF-13 are associated with velocity variations and show the presence of carbonate deposits. The slope-front deposits and fan facies suggest deep-water slope fan facies and delta fan facies.

The following conclusions are drawn regarding the depositional settings of the Lake Fuxian basin (Fig. 9b);

(a) The sediment source originated from highlands, which were triggered by high seismic activity. Different geological episodes significantly controlled the clastic sediment depositional system. From a regional geological perspective, seismic facies, sedimentary sequences, and tectonic events in the lake basin and its surroundings uniformly triggered highly intense seismic activity, which governed the large geological basins in the region.

(b) Lake Fuxian is the largest intermountain basin and the deepest graben in the Yunnan Plateau region. The dominant sedimentary units were deposited in deep calcareous sediments and shallow alluvial as well as lacustrine sediments.

(c) They consist of open to marginal lacustrine deposits, breccia deposits and fluvial deposits. The upper units (probably Quaternary and Neogene) feature sequences of fan delta deposits, interbedded marginal lacustrine deposits, and fluvial deposits, whereas thick coarse-grained fan-delta deposits are interfingered at the foot of the main relief with fluvial-lacustrine deposits.

(d) The two distinct disconformable sedimentary units represent the pre-syngenetic tectonic activity in the basin. The low-slip margin fine sediment rock units are pre-tectonic, while the high-slip margin coarse sediments are syngeneic due to high tectonic activity.

6 Conclusions

The main conclusions are as follows:

1. Five seismic sequences were interpreted. The oldest sequence (Sq-5) at L8 shows that the clinoforms terminate against the seismic section and that the sedimentation of the sedimentary cover can extend beyond the section to ~50 m to ~100 m. The deeper sequences (Sq-5 and Sq-4)

show deposition during the prograding late lowstand and early lowstand stages. The deepest clinoforms show that the lowest lake level of the lake basin was ~210 m during late lowstand settings. Sq-3 shows the transition phase of transgressive stages. Several mound-shaped reflections in Sq-4 and Sq3 provide evidence of backstepping deltaic sedimentation, suggesting littoral and postlittoral zonations. Sq-2 shows the deposition of sediments during late highstand stages, during which several flooding surfaces were deposited, resulting in further retrogradation. However, Sq-1 provides insights into the initial phases of hemipelagic deposition in a profundal paleoenvironment.

2. It is inferred that the coastline migrated nearly 1.5 km on each side horizontally in the southern basin, approximately 2 km toward the ESE region in the central basin, and approximately 19 km to the SSW region in the northern basin at its current location.

3. The sedimentary thickness of the basin is highly variable. The maximum thickness of the sedimentation toward the southern basin is ~303 m at L1, ~348 m toward the central basin at L4, and ~1238 m toward the northern basin at L10-2.

4. The lake sediments toward the southern basin underwent more tectonic activity since the disruption and reflection patterns were more chaotic and dispersed at L2. In general, tectonic activity played an important role in crustal extension and the formation of horst and graben structures within the lake basin.

5. The lake basin can be characterized into three main depositional patterns that incorporate alluvial delta plains, alluvial fans, and terraces. The U- and V-shaped erosional patterns show the fluvial nature of lake sediments that are linked with paleochannels and associated levees. However, a mound-shaped pattern is linked with backstopping progradational settings and velocity variations.

6. The major geological controlling factor within the Lake Fuxian basin is crustal tectonics that related to the parallel normal faulting, which causes rifting and crustal extension and the formation of horst and graben structures. Secondary factors include fill and subsidence, SAR in relation to lake-level variations and sediment thickness distribution.

7 Recommendations

The proposed study lays the foundation for the Lake Fuxian drilling project. Since this pioneer study to utilized multichannel seismic refection profiles, the precision of the interpretations among seismic sequences and core lithologies must be checked by actual drilling activity.

Data availability   The data analyzed in this study are subject to the following licenses/restrictions: The data are confidential and cannot be made available. Requests to access these datasets should be directed to the corresponding authors.

Declarations

Conflict of interest   The authors declare no conflicts of interest.

Ethical approval   Not applicable.

Consent to publish   Not applicable.

References

Adams EW, Schlager W, Anselmetti FS (2001) Morphology and curvature of delta slopes in Swiss lakes: lessons for the interpretation of clinoforms in seismic data. Sedimentology 48(3):661–679

Anees A, Wanzhong S, Ashraf U, Qinghai X (2019) Channel identification using 3D seismic attributes in lower Shihezi Formation of Hangjinqi area, northern Ordos Basins, China. J. Appl. Geophys. 163:139–150

Anees A, Zhang H, Ashraf U, Wang R, Liu K, Mangi HN, Shi W (2022) Identification of favorable zones of gas accumulation via fault distribution and sedimentary facies: insights from Hangjinqi Area, Northern Ordos Basin. Front Earth Sci 9:1375

Ashraf U, Zhu P, Yasin Q, Anees A, Imraz M, Mangi HN, Shakeel S (2019) Classification of reservoir facies using well log and 3D seismic attributes for prospect evaluation and field development: a case study of Sawan gas field, Pakistan. J Petrol Sci Eng 175:338–351

Ashraf U, Zhang H, Anees A, Mangi HN, Ali M, Zhang X, Tan S (2021) A core logging, machine learning and geostatistical modeling interactive approach for subsurface imaging of lenticular geobodies in a clastic depositional system, SE Pakistan. Nat Resour Res 30(3):2807–2830

Barrpso GF, Goncalves MA, Garcia FC (2015) The morphometry of Lake Palmas, a deep natural Lake in Brazil. PLoS One 9:1–13

Bohacs KM, Carroll AR, Neal JE, Mankiewicz PJ, Gierlowski-Kordesch EH, Kelts KR (2000) Lake-basin type, source potential, and hydrocarbon character: an integrated sequence-stratigraphic-geochemical framework. Lake Basins through Space Time AAPG Stud Geol 46:3–34

Bureau of Geology and Mineral Resources of Yunnan Province (1990) Regional geological annals of Yunnan Province. Geological Publishing House, Beijing, pp 659–727. (**in Chinese with brief text in English**)

Butch JL (1996) Compositional and textural analysis of sandy sediments across two rift lake deltas: Songwe-Kiwira and Dwangwa deltas, Lake Malawi, East Africa, Doctoral dissertation, University of North Carolina at Chapel Hill

Cheng N, Liu L, Hou Z, Wu J, Wang Q (2020) Pollution characteristics and risk assessment of surface sediments in nine plateau lakes of Yunnan Province. IOP Conf Ser Earth Environ Sci 467(1):012166

Cheng J, Xu X, Ren J, Zhang S, Wu X (2021) Probabilistic multi-segment rupture seismic hazard along the Xiaojiang fault zone, Southeastern Tibetan Plateau. J Asian Earth Sci 221:104940

Colman SM, Karabanov EB, Nelson CH III (2003) Quaternary sedimentation and subsidence history of Lake Baikal, Siberia, based on seismic stratigraphy and coring. J Sediment Res 73(6):941–956

Cui YD, Liu XQ, Wang HZ (2008) Macrozoobenthic community of Fuxian Lake, the deepest lake of southwest China. Limnologica 38(2):116–125

Dai X, Zhou Y, Ma W, Zhou L (2017) Influence of spatial variation in land-use patterns and topography on water quality of the rivers inflowing to Fuxian Lake, a large deep lake in the plateau of southwestern China. Ecol Eng 99:417–428

Dietze E, Hartmann K, Diekmann B, IJmker J, Lehmkuhl F, Opitz S, Borchers A (2012) An end-member algorithm for deciphering modern detrital processes from lake sediments of Lake Donggi Cona, NE Tibetan Plateau, China. Sediment Geol 243:169–180

Flannery JW, Rosendahl BR (1990) The seismic stratigraphy of Lake Malawi, Africa: implications for interpreting geological processes in lacustrine rifts. J Afr Earth Sci (middle East) 10(3):519–548

Gao Y, Zhang H, Zhang X, Duan L, Lei G, Pu Y, Anee A (2024) Early-middle Holocene high lake levels of Rinqen Shubtso on the southern Tibetan Plateau and the formation mechanisms. Sci Total Environ 906:167702

Gierlowski-Kordesch EH, Kelts KR (2000) Preface. In: Gierlowski-Kordesch E, Kelts K (eds) Lake basins through space and time, AAPG Studies in Geology. vol 46. pp 3–8

Guo P, Han Z, Dong S, Mao Z, Hu N, Gao F, Billi A (2021) Latest quaternary active faulting and paleoearthquakes on the southern segment of the Xiaojiang Fault Zone, SE Tibetan Plateau. Lithosphere 2021(1)

Hutchinson DR, Golmshtok AJ, Zonenshain LP, Moore TC, Scholz CA, Klitgord KD (1992) Depositional and tectonic framework of the rift basins of Lake Baikal from multichannel seismic data. Geology 20(7):589–592

Jiang H, Zhong N, Li Y, Ma X, Xu H, Shi W, Nie G (2017) A continuous 13.3-ka record of seismogenic dust events in lacustrine sediments in the eastern Tibetan Plateau. Sci Rep 7:15686. https://doi.org/10.1038/s41598-017-16027-8

Johnson TC (1984) Sedimentation in large lakes. Annu Rev Earth Planet Sci 12(1):179–204

Johnson TC, Scholz CA, Talbot MR, Kelts K, Ricketts RD, Ngobi G, McGill JW (1996) Late Pleistocene desiccation of Lake Victoria and rapid evolution of cichlid fishes. Science 273(5278):1091–1093

Johnson TC, Brown ET, McManus J, Barry S, Barker P, Gasse F (2002) A high-resolution paleoclimate record spanning the past 25,000 years in southern East Africa. Science 296(5565):113–132

Jun S, Yipeng W, Fangmin S (2003) Characteristics of the active Xiaojiang fault zone in Yunnan, China: a slip boundary for the southeastward escaping Sichuan-Yunnan Block of the Tibetan Plateau. J Asian Earth Sci 21(10):1085–1096

Li X, Bai D, Ma X, Chen Y, Varentsov IM, Xue G, Lozovsky I (2019a) Electrical resistivity structure of the Xiaojiang strike-slip fault system (SW China) and its tectonic implications. J Asian Earth Sci 176:57–67

Li T, Zhang H, Cai M, Chang F, Hu J, Duan L, Zhang Y (2019b) The composition of carbonate matters in the sediments from Lake Fuxian and significance

of paleoclimate and water level changes. Quat Sci 39(3):642–654

Liu E, Zhang E, Li K, Nath B, Li Y, Shen J (2013a) Historical reconstruction of atmospheric lead pollution in central Yunnan province, southwest China: an analysis based on lacustrine sedimentary records. Environ Sci Pollut Res 20(12):8739–8750

Liu G, Liu Z, Chen F, Zhang Z, Gu B, Smoak JM (2013b) Response of the cladoceran community to eutrophication, fish introductions and degradation of the macrophyte vegetation in Lake Dianchi, a large, shallow plateau lake in southwestern China. Limnology 14(2):159–166

Liu G, Liu Z, Gu B, Smoak JM, Zhang Z (2014) How important are trophic state, macrophyte and fish population effects on cladoceran community? A Study in Lake Erhai. Hydrobiologia 736(1):189–204

Liu G, Liu Z, Smoak JM, Gu B (2015) The dynamics of cladoceran assemblages in response to eutrophication and planktivorous fish introduction in Lake Chenghai, a plateau saline lake. Quatern Int 355:188–193

Lyons RP, Scholz CA, Buoniconti MR, Martin MR (2011) Late quaternary stratigraphic analysis of the Lake Malawi Rift, East Africa: an integration of drill-core and seismic-reflection data. Palaeogeogr Palaeoclimatol Palaeoecol 303(1–4):20–37

McGlue MM, Lezzar KE, Cohen AS, Russell JM, Tiercelin JJ, Felton AA, Nkotagu HH (2008) Seismic records of late Pleistocene aridity in Lake Tanganyika, tropical East Africa. J Paleolimnol 40(2):635–653

McGlue MM, Scholz CA, Karp T, Ongodia B, Lezzar K-E (2006) Facies architecture of flexural margin lowstand delta deposits in Lake Edward, East African Rift: Constraints from seismic reflection imaging. J Sed Re 76:942–958

Menking KM, Bischoff JL, Fitzpatrick JA, Burdette JW, Rye RO (1997) Climatic/hydrologic oscillations since 155,000 yr BP at Owens Lake, California, reflected in abundance and stable isotope composition of sediment carbonate. Quatern Res 48(1):58–68

Messager ML, Lehner B, Grill G, Nedeva I, Schmitt O (2016) Estimating the volume and age of water stored in global lakes using a geo-statistical approach. Nat Commun 7(1):1–11

Nanjing Institute of Geography and Limnology, Chinese Academy of Sciences (1990) Fuxian Lake. Ocean Press, Beijing, pp 1–7. (**in Chinese**)

Porębski SJ, Steel RJ (2006) Deltas and sea-level change. J Sediment Res 76(3):390–403

Schlaf J, Randen T, Sønneland L (2005) Introduction to seismic texture. In: Mathematical methods and modelling in hydrocarbon exploration and production. Springer, Berlin, Heidelberg, pp 3–21

Scholz CA (1995) Deltas of the Lake Malawi Rift, East Africa: Seismic expression and exploration implications. AAPG Bull 79:1679–1697

Scholz CA, Rosendahl BR, Scott DL (1990) Development of coarse-grained facies in lacustrine rift basins: examples from East Africa. Geology 18(2):140–144

Sladen C (2012) Lake systems. Reg Geol Tecton Princ Geol Anal 1:407

Soreghan MJ, Scholz CA, Wells JT (1999) Coarse-grained deep-water sedimentation along a border fault margin of Lake Malawi, Africa: seismic stratigraphic analysis. J Sed Res 69:832–846

Strecker U, Steidtmann JR, Smithson SB (1999) A conceptual tectonostratigraphic model for seismic facies migrations in a fluvio-lacustrine extensional basin. AAPG Bull 83(1):1320–1336

Sun QF, Shen CM, Wang M, Meng HW, Zhang HC (2018) Pollen/charcoal record over the past 13,300 years from Fuxian lake in the Yunnan-Guizhou Plateau. Acta Paleontol Sin 57(2):249–259

Torrado L, Carvajal-Arenas LC, Mann P, Bhattacharya J (2020) Integrated seismic and well-log analysis for the exploration of stratigraphic traps in the Carbonera Formation, Llanos foreland basin of Colombia. J S Am Earth Sci 104:102607

Trinchero E (2000) The fault shadow problem as an interpretation pitfall. Lead Edge 19(2):132–135

Wang C, Lou H, Wang X, Qin J, Yang R, Zhao J (2009) Crustal structure in Xiaojiang fault zone and its vicinity. Earthq Sci 22(4):347–356

Wang XL, Yang H, Ding ZY, Yang BJ, Zhang ML (2011) Modern sedimentation rates of Fuxian Lake by 210Pb and 137Cs dating. Acta Geogr Sin 66:1551–1561

Wang X, Yang H, Gu Z, Zhang M, Yang B (2018) A century of change in sediment accumulation and trophic status in Lake Fuxian, a deep plateau lake of Southwestern China. J Soils Sediments 18(3):1133–1146

Wang J, He Z, Li L (2021a) Palaeoseismic records in lacustrine sediments—a case study of the Daqingshan piedmont fault and Hasuhai Lake in Inner Mongolia, China. Basin Res 33(1):681–704

Wang X, Yang H, Kitch JL, Liu J, Xue B (2021b) Grain-size characteristics in lake Fuxian sediments: implication for dry-humid transformation of Indian summer monsoon over the past 150 years. J Asian Earth Sci X 6:100073

Wartes MA, Carroll AR, Greene TJ, Cheng K, Ting H (2000) AAPG studies in geology# 46, Chapter 8: Permian Lacustrine Deposits of Northwest China

Wells JT, Scholz CA, Soreghan MJ (1999) Processes of sedimentation on a lacustrine border-fault margin; interpretation of cores from Lake Malawi, East Africa. J Sediment Res 69(4):816–831

Yin J, Zhang W, Liu T, Ma S, Liang Q, Liu S (2021) Organic carbon burial and quasi-periodic environmental changes in the Indian summer monsoon region during the Holocene. CATENA 206:105462

Zeng HA, Wu JL (2009) Sedimentary records of heavy metal pollution in Fuxian Lake, Yunnan Province, China: intensity, history, and sources. Pedosphere 19(5):562–569

Zhang E, Liu E, Shen J, Cao Y, Li Y (2012) One century sedimentary record of lead and zinc pollution in Yangzong Lake, a highland lake in southwestern China. J Environ Sci 24(7):1189–1196

Zhang Y, Li K, Zhou Q, Chen L, Yang X, Zhang H (2021a) Phytoplankton responses to solar UVR and its combination with nutrient enrichment in a plateau oligotrophic Lake Fuxian: a mesocosm experiment. Environ Sci Pollut Res 28(23):29931–29944

Zhang LT, Yang XL (2012) Chinese lakes. Bengtsson L, Herschy RW, Fairbridge RW(eds) Encyclopedia of lakes and reservoirs. Springer Science Business Media, Berlin, pp 156–160

Zhang X, Zhang H, Chang F, Ashraf U, Wu H, Peng W, Duan L (2021b) Sedimentary grain-size record of Holocene runoff fluctuations in the Lake Lugu watershed, SE Tibetan Plateau. Holocene 31(3):346–355

Zhang X, Zhang H, Chang F, Xie P, Li H, Wu, H, Ouyang C, Liu F, Peng W, Zhang Y, Liu Q, Duan L, Ashraf U (2021) Long-range transport of aeolian deposits during the last 32 kyr inferred from rare earth elements and grain-size analysis of sediments from Lake Lugu, Southwestern China. Palaeogeogr Palaeoclimatol Palaeoecol 567:110248

Zhuo Y, Zeng W, Cui D, Ma B, Xie Y, Wang J (2021) Spatial-temporal variation, sources and driving factors of organic carbon burial in rift lakes on Yunnan-Guizhou plateau since 1850. Environ Res 201:111458